

## Experimental characterization of the post-cracking response in Hybrid Steel/Polypropylene Fiber-Reinforced Concrete

Antonio Caggiano<sup>a</sup>, Serena Gambarelli<sup>b</sup>, Enzo Martinelli<sup>c,\*</sup>, Nicola Nisticò<sup>b</sup>, Marco Pepe<sup>c</sup>

<sup>a</sup> Nat. Scientific and Technical Research Council (CONICET) & University of Buenos Aires (UBA), Ciudad Autónoma de Buenos Aires, Argentina

<sup>b</sup> Department of Structural and Geotechnical Engineering, Sapienza University of Rome, via Eudossiana 18, 00184 Roma, Italy

<sup>c</sup> Department of Civil Engineering, University of Salerno, via Giovanni Paolo II 132, 84084 Fisciano, SA, Italy

### HIGHLIGHTS

- This paper deals with Hybrid Steel/Polypropylene Fiber-Reinforced Concrete (HyFRC).
- It focuses on five HyFRC mixtures made with an invariant volume fraction of fibers.
- Experimental results from tests under both compression and bending are reported.
- Steel fibers mainly contribute to strain re-hardening force-crack response.
- Specimens with more polypropylene fibers exhibited a less variable response.

### ARTICLE INFO

#### Article history:

Received 10 July 2016

Received in revised form 16 August 2016

Accepted 19 August 2016

Available online 6 September 2016

#### Keywords:

Fiber-Reinforced Concrete

Hybrid FRC

Steel fibers

Polypropylene fibers

Ductility

Four-point bending

### ABSTRACT

This paper presents and discusses the results of experimental tests performed on concrete specimens internally reinforced with polypropylene and steel fibers. Specifically, samples of five mixtures (plus a reference plain concrete), characterized by the same total volume of fibers, but different fractions of polypropylene and steel fibers, were tested under compression and in bending. This study was aimed to clarify the influence of different combinations of these fibers on the resulting fracture behavior of Hybrid Fiber-Reinforced Concrete (HyFRC). As expected, the results obtained from compression tests highlighted a negligible influence of fibers in terms of strength and, hence, FRC specimens exhibited a post-peak response more ductile than the reference ones. Conversely, the overall shape of the stress-crack-opening-displacement curves of HyFRC tested in bending was highly influenced by the type of fibers. On the one hand, FRC specimens made of only polypropylene fibers exhibited an excellent post-cracking toughness for the small crack opening ranges of relevance for the Serviceability Limit State, while an apparent decay was observed in terms of post-cracking response, especially at wide crack openings. On the other hand, a marked re-hardening response was observed in the post-cracking behavior for specimens with higher percentage of steel fibers; however, at the same time, the corresponding results showed a relevant scatter.

© 2016 Elsevier Ltd. All rights reserved.

### 1. Introduction

Fiber-Reinforced Cementitious Composites (FRCCs), obtained by mixing short fibers within conventional cement-based matrices (i.e., mortar or concrete), can be considered as structural materials featuring both post-cracking tensile strength higher than the corresponding matrices and enhanced toughness (in terms of absorbed

strain energy) due to the bridging actions developed by fibers across the opening crack surfaces [1,2]. Among these materials, Fiber-Reinforced Concrete (FRC) is commonly used for structural purposes, such as strengthening existing members [3] and controlling crack opening in new ones [4].

Main concepts behind the structural rules for FRC structural design are commented in several studies and have been well focused in [5]. Among the high performance properties of FRC, the most appealing is its “re-hardening” capacity in tension and bending: a comprehensive classification between strain-hardening (multi-cracking) vs. strain-softening composites has been reported in [6]. It is worth noticing that the bond behavior

\* Corresponding author.

E-mail addresses: [acaggiano@fi.uba.ar](mailto:acaggiano@fi.uba.ar) (A. Caggiano), [serena.gambarelli@uniroma1.it](mailto:serena.gambarelli@uniroma1.it) (S. Gambarelli), [e.martinelli@unisa.it](mailto:e.martinelli@unisa.it) (E. Martinelli), [nicola.nistico@uniroma1.it](mailto:nicola.nistico@uniroma1.it) (N. Nisticò), [mapepe@unisa.it](mailto:mapepe@unisa.it) (M. Pepe).



**Table 1**

Relevant properties of fibers [33,34].

Fibers		Diameter [mm]	Length [mm]	Tensile strength [MPa]	Elastic Modulus [GPa]
Steel (S)	WIRAND® FS7	0.550	33	>1200	210
Polypropylene (P)	FIBROMAC® 12	0.032	12	400–500	3.5–3.9

**Table 2**

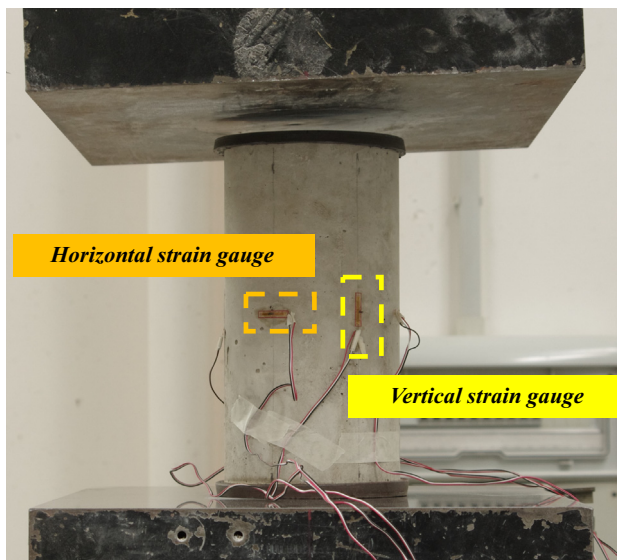
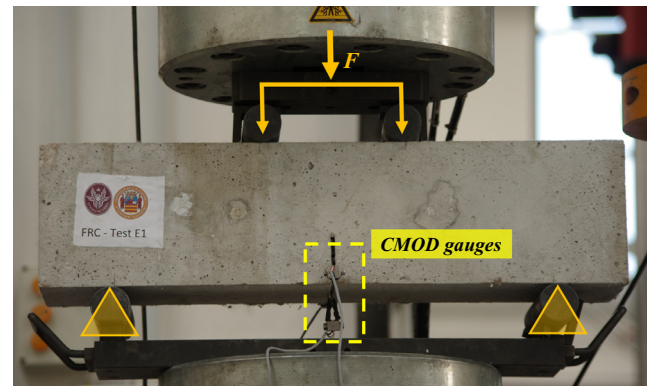
FRC mixtures: composition of the fiber phase.

Mixture	Steel fibers (S)		Polypropylene fibers (P)	
	Volume fraction [%]	In weight [kg/m <sup>3</sup> ]	Volume fraction [%]	In weight [kg/m <sup>3</sup> ]
HySP-FRC-0.75-0	0.75	60	–	–
HySP-FRC-0.55-0.20	0.55	45	0.2	1.7
HySP-FRC-0.375-0.375	0.375	30	0.375	3.4
HySP-FRC-0.20-0.55	0.2	15	0.55	5.1
HySP-FRC-0-0.75	–	–	0.75	6.8

**Table 3**

Concrete mix composition.

Material	Dosage [kg/m <sup>3</sup> ]
Cement 42.5	420
Water	210
Sand (0–4 mm)	800
Aggregates (6–12 mm)	800

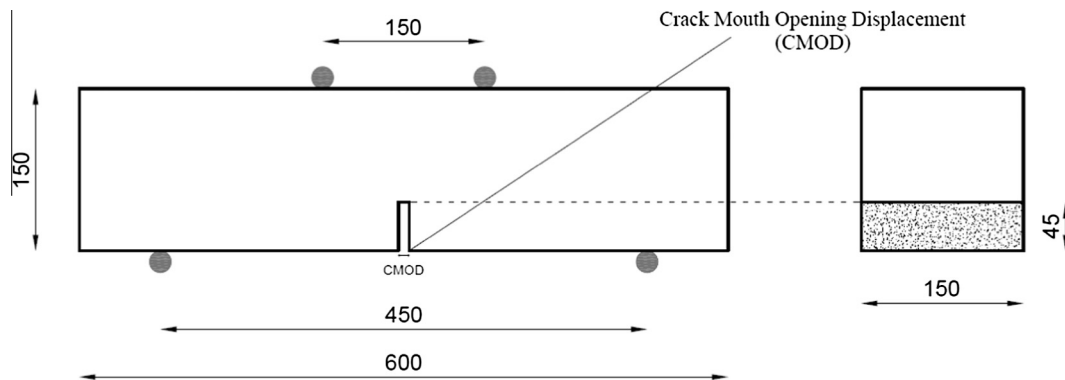
**Fig. 2.** Experimental set-up for the uniaxial compressive tests.**Fig. 4.** Experimental set-up for the 4PB tests.

[37] were also considered. Particularly, the displacement rate was set to 0.005 mm/min and three displacement transducers were placed inside the notch to monitor the so-called Crack Mouth Opening Displacement (CMOD), which is defined as the relative displacement between the two points at the bottom sides of the notch (Fig. 3). Then, Fig. 4 shows the aforementioned experimental setup.

### 3. Results and discussion

#### 3.1. Uniaxial compression tests

Fig. 5 shows the results of the tests in terms of uniaxial compressive strength; error bars indicate the scatter between the

**Fig. 3.** Geometry of the notched beams.

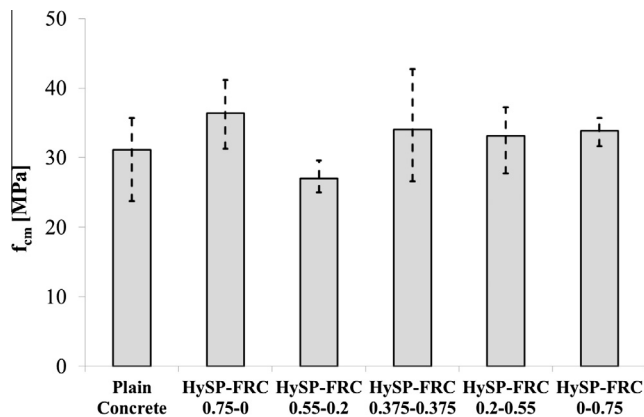


Fig. 5. Cylindrical compressive strengths for HySP-FRCs.

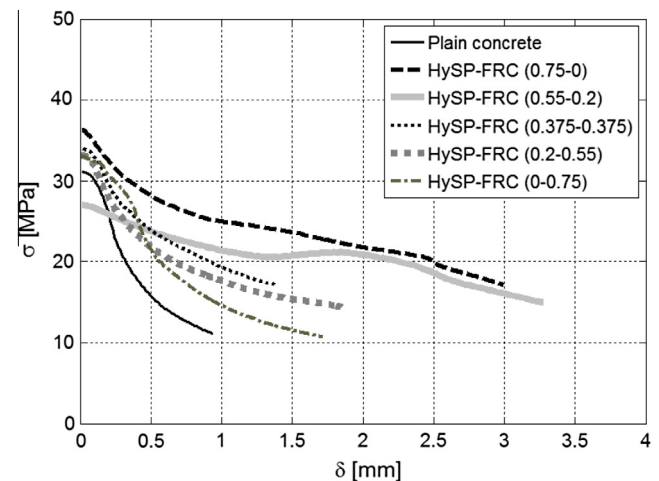


Fig. 6. Compression post-peak behavior: average axial stress vs displacement for HySP-FRCs.

minimum and the maximum values obtained for each mixture. For the sake of clarity, Table 4 reports the numerical values of compressive strength obtained in all tests.

As expected from similar studies available in the literature [9,17,31], the tests on HySP-FRC specimens led to results fairly close to the output obtained for the reference plain concrete. The maximum variation was measured for the specimens reinforced with only steel fibers (HySP-FRC-0.75-0): a percentage increment of about 15% was actually observed.

Based on these observations, it may be concluded that the resulting compressive strength of the tested HyFRC is mainly governed by the composition of the concrete matrix. Conversely, as it is well-known, fibers play an important role in controlling the post-peak regime, as they “bridge” the opening cracks. A less softening response in the post-peak region, with respect to plain concrete, characterizes the HyFRC specimens, especially those with higher content of steel fibers, as can be appreciated in Fig. 6, which plots the average axial stress ( $\sigma$ ) vs displacement ( $\delta$ ) curves for all the analyzed mixtures.

Each one of the curves reported in Fig. 6 was obtained by averaging the stresses of the tested samples (3 cylinders for the HySP-FRCs and 6 for plain reference concrete): Fig. 7 reports the individual  $\sigma$ - $\delta$  curves obtained in each test.

Finally, it is worth highlighting that, in these curves,  $\delta$  represents the vertical displacement imposed by the testing machine: the curves report the post-peak behavior, starting from the maximum measured stress.

### 3.2. Four-point bending tests

The 4PB tests were executed on three specimens for each mixture. The typical failure mode of a fiber-reinforced specimen (i.e., HySP-FRC-0.75-0) is shown in Fig. 8. The vertical load (F) and the corresponding Crack Mouth Opening Displacement (CMOD) were monitored during each test. More specifically, the

CMOD was evaluated as the average of the three acquired measurements.

The F-CMOD curves obtained for each mixture are shown in Figs. 9a–9e. For a given mixture, the scatter between the curves is very low, confirming the reliability of the acquired data and the symmetry of the loading process.

For each mixture, an averaged Force-Displacement curve has been evaluated by calculating the mean value of the three CMODs measured with the transducers. Thus, a unique curve (F-CMOD<sub>m</sub>) can be obtained also averaging the forces (of the three tested samples) corresponding to a given CMOD level.

The F-CMOD<sub>m</sub> curves evaluated for all the analyzed mixtures are shown in Fig. 10: on each graph, the black line represents the average response of the three tests, whereas the grey area highlights the scatter between the results. This scatter is usually due to various effects (e.g. the irregular space distribution of fibers, variable number and orientation of fibers crossing the crack surface, etc.), which contribute to the natural uncertainty of the experimental behavior.

However, the results generally point out that the post-cracking response of FRC specimens made with only steel fibers is characterized by significant toughness (Fig. 10b), as a result of the significant bridging action exploited by those fibers, which is not present in plain concrete (Fig. 10a).

Furthermore, the effect of replacing part of steel fibers with an equivalent volume of polypropylene fibers, can be easily caught by analyzing Fig. 11. In the post-cracking behavior of HySP-FRC, the following stages can be identified:

Stage I) an early post-peak branch with CMOD<sub>m</sub> lower than 0.8 mm;

Stage II) characterized by CMOD<sub>m</sub> in between 0.8 and 1 mm;

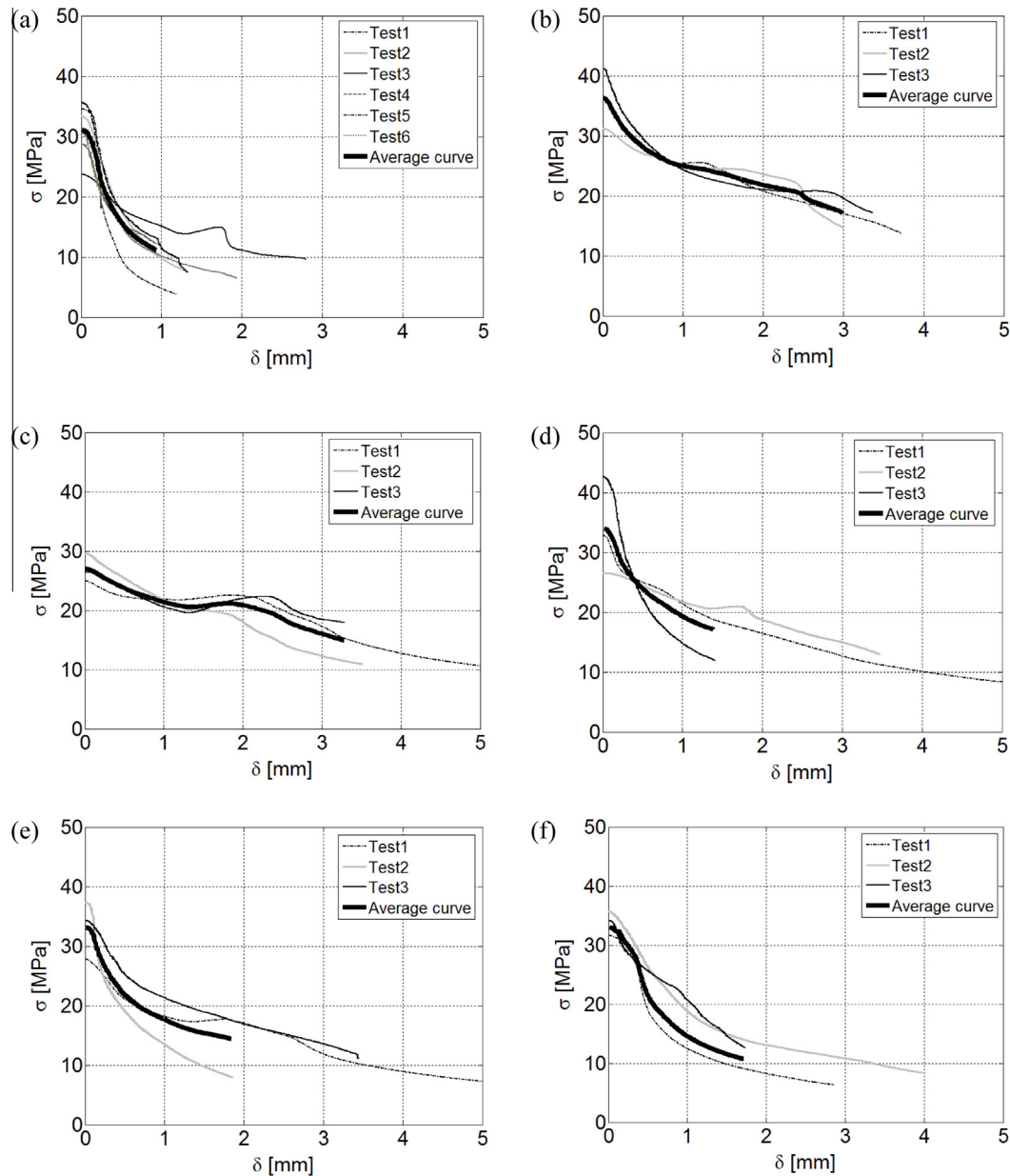
Stage III) with crack opening displacements greater than 1 mm.

Table 4

Experimental results for HySP-FRC specimens tested in compression.

Mixture	Test 1 [MPa]	Test 2 [MPa]	Test 3 [MPa]	Test 4 [MPa]	Test 5 [MPa]	Test 6 [MPa]	$f_{cm}$ [MPa]	Err <sup>+</sup> [MPa]	Err <sup>-</sup> [MPa]
Plain Concrete	34.57	33.406	23.722	30.59	35.675	28.711	31.11	4.56	7.39
HySP-FRC-0.75-0	36.64	31.287	41.177	–	–	–	36.37	4.81	5.08
HySP-FRC-0.55-0.2	24.99	29.598	26.445	–	–	–	27.01	2.59	2.02
HySP-FRC-0.375-0.375	32.89	26.595	42.679	–	–	–	34.05	8.63	7.46
HySP-FRC-0.2-0.55	27.75	37.257	34.289	–	–	–	33.10	4.16	5.35
HySP-FRC-0-0.75	31.66	35.712	34.169	–	–	–	33.848	1.86	2.18





**Fig. 7.** Compression post-peak behavior in terms of axial stress vs vertical displacement: a) Plain concrete; b) HySP-FRC-0.75-0; c) HySP-FRC-0.55-0.2; d) HySP-FRC-0.375-0.375; e) HySP-FRC-0.2-0.55; f) HySP-FRC-0-0.75.



**Fig. 8.** Typical failure mode (HySP-FRC-0.75-0).

In Stage I, the slope of the descending (softening) branch is more pronounced for the mixtures with higher content of S fibers, denoting a more delayed activation of such fibers in comparisons to the P-fibers: this is mainly due to the lower number of S fibers corresponding to the same volume of P ones.

In Stage II, steel fibers begin to give a significant contribution, while the P-ones tend to lose their action mainly due to either/both debonding or/and tensile failure mechanisms. Therefore, on the one hand, a re-hardening response can be observed for the specimens characterized by a high amount of S-fibers, while, on the other hand, a crack-softening behavior was obtained for specimens with a predominant percentage of P-fibers (Fig. 11).

In Stage III, the activated P fibers reach their maximum bond strength and react with a constant friction force while a further bridging effect is still offered by S fibers, which actually results in a hardening response as the crack opening increases.

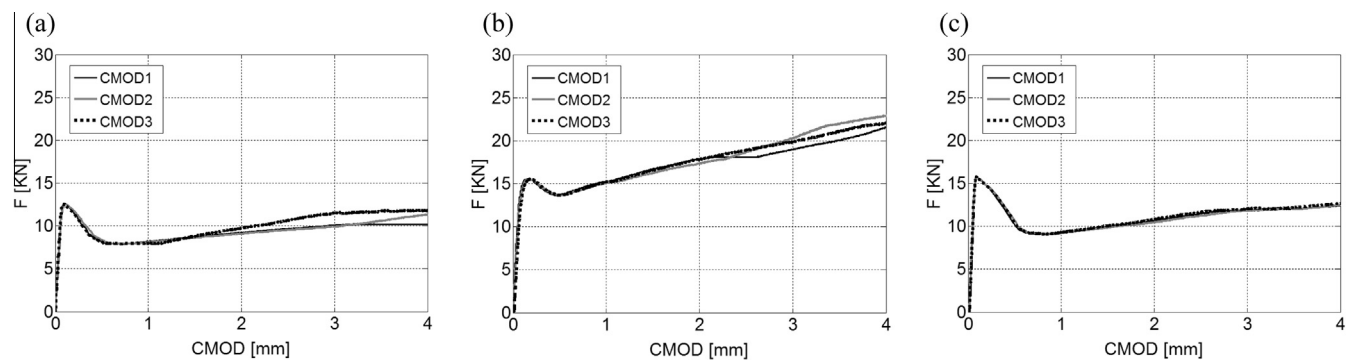


Fig. 9a. HySP-FRC-0.75-0: a) Test1, b) Test2 and c) Test3.

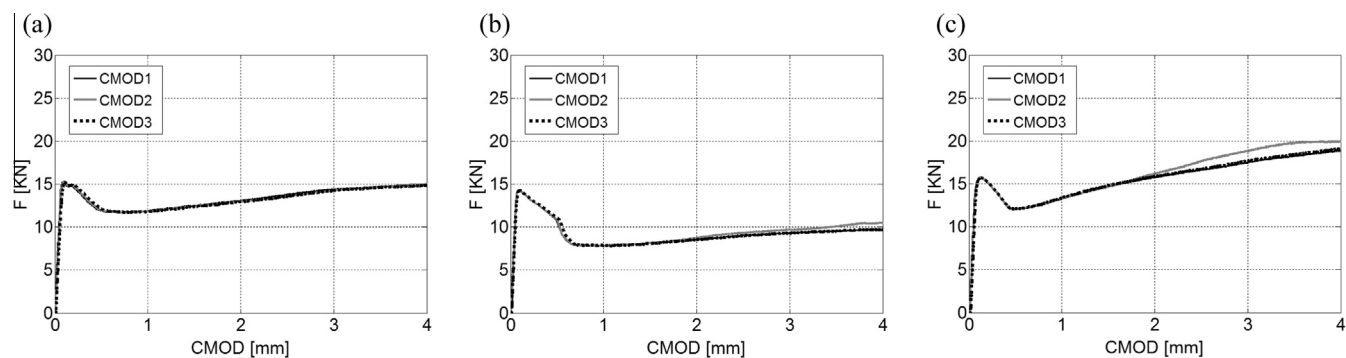


Fig. 9b. HySP-FRC-0.55-0.2: a) Test1, b) Test2 and c) Test3.

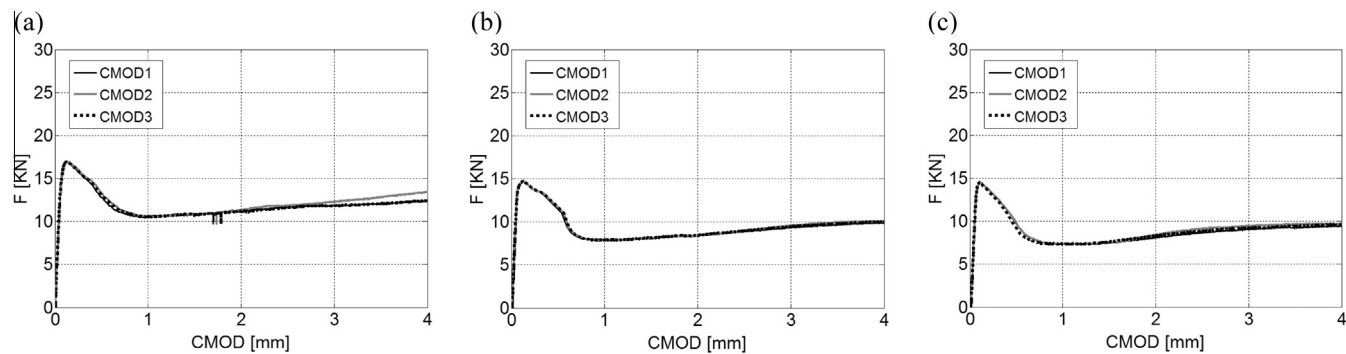


Fig. 9c. HySP-FRC-0.375-0.375: a) Test1, b) Test2 and c) Test3.

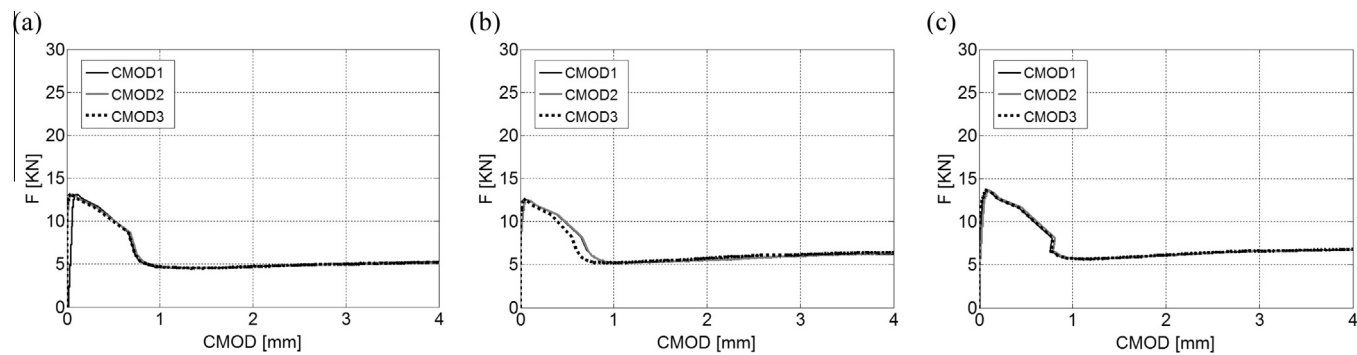


Fig. 9d. HySP-FRC-0.2-0.55: a) Test1, b) Test2 and c) Test3.

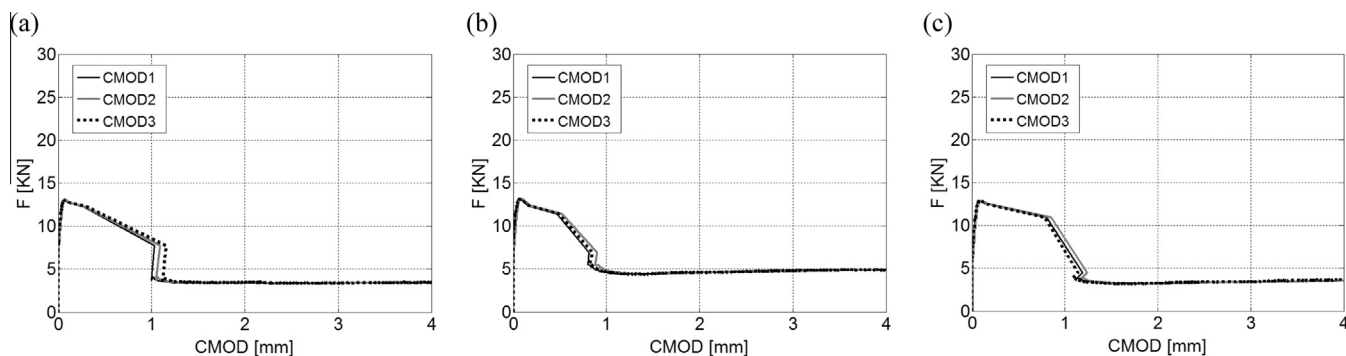


Fig. 9e. HySP-FRC-0-0.75: a) Test1, b) Test2 and c) Test3.

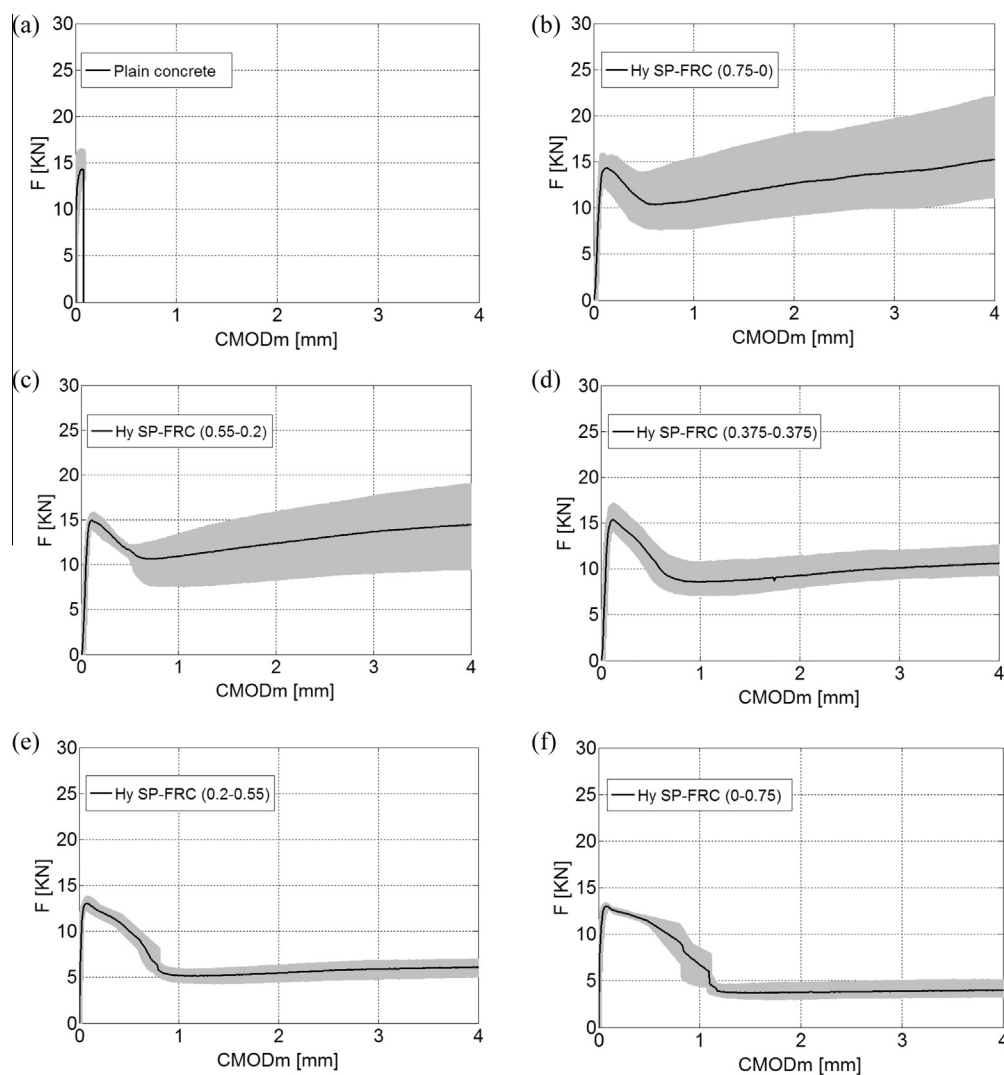


Fig. 10. F vs CMOD<sub>m</sub>: a) Plain concrete, b) HySP-FRC-0.75-0, c) HySP-FRC-0.55-0.2, d) HySP-FRC-0.375-0.375, e) HySP-FRC-0.2-0.55 and f) HySP-FRC-0-0.75.

Another important evidence of the experimental results is that the scatter between experimental results reduces significantly in specimens with higher contents of polypropylene fibers. This is most likely due to both the higher number of P fibers replacing an equal volume of S fibers and the higher aspect ratio of the P fibers with respect to the S fibers. Thus, a more regular distribution of polypropylene fibers was observed throughout the cracked surface in all tested specimens compared to the usual non-regular

distribution of steel fibers. Table 5 summarizes the main parameters evaluated through the experimental test results.

More specifically, it reports the values obtained for:

- 1)  $F_{max}$ , representing the maximum force achieved in the ascending cracking phase;
- 2)  $CMOD_{m,Fmax}$ , representing the  $CMOD_m$  corresponding to  $F_{max}$ ;





- [18] L.G. Sorelli, A. Meda, G.A. Plizzari, Bending and uniaxial tensile tests on concrete reinforced with hybrid steel fibers, *J. Mater. Civ. Eng.* 17 (5) (2005) 519–527.
- [19] N.A. Libre, M. Shekarchi, M. Mahoutian, P. Soroushian, Mechanical properties of hybrid fiber reinforced lightweight aggregate concrete made with natural pumice, *Constr. Build. Mater.* 25 (5) (2011) 2458–2464.
- [20] W. Yao, J. Li, K. Wu, Mechanical properties of hybrid fiber-reinforced concrete at low fiber volume fraction, *Cem. Concr. Res.* 33 (1) (2003) 27–30.
- [21] E. Dawood, M. Ramli, Mechanical properties of high strength flowing concrete with hybrid fibers, *Constr. Build. Mater.* 28 (1) (2012) 193–200.
- [22] M. Sahmaran, I. Yaman, Hybrid fiber reinforced self-compacting concrete with a high-volume coarse fly ash, *Constr. Build. Mater.* 21 (1) (2007) 150–156.
- [23] B. Akcay, M. Tasdemir, Mechanical behaviour and fiber dispersion of hybrid steel fiber reinforced self-compacting concrete, *Constr. Build. Mater.* 28 (1) (2012) 287–293.
- [24] Y. Ding, C. Azevedo, J. Aguiar, S. Jalali, Study on residual behaviour and flexural toughness of fiber cocktail reinforced self compacting high performance concrete after exposure to high temperature, *Constr. Build. Mater.* 26 (1) (2012) 21–31.
- [25] R. de Montaignac, B. Massicotte, J.-P. Charron, A. Nour, Design of SFRC structural elements: post-cracking tensile strength measurement, *Mater. Struct.* 45 (4) (2012) 609–622.
- [26] J. Michels, R. Christen, D. Waldmann, Experimental and numerical investigation on postcracking behavior of steel fiber reinforced concrete, *Eng. Fract. Mech.* 98 (2013) 326–349.
- [27] L. Facconi, F. Minelli, G. Plizzari, Steel fiber reinforced self-compacting concrete thin slabs—Experimental study and verification against Model Code 2010 provisions, *Eng. Struct.* 122 (2016) 226–237.
- [28] F. Soltanzadeh, A.E. Behbahani, H. Mazaheripour, J.A.O. Barros, Shear resistance of SFRCSCC short-span beams without transversal reinforcements, *Compos. Struct.* 139 (2016) 42–61.
- [29] F. de Andrade Silva, B. Mobasher, R.D. Toledo Filho, Fatigue behavior of sisal fiber reinforced cement composites, *Mater. Sci. Eng., A* 527 (21–22) (2010) 5507–5513.
- [30] A.G. Graeff, K. Pilakoutas, K. Neocleous, M.V.N. Peres, Fatigue resistance and cracking mechanism of concrete pavements reinforced with recycled steel fibers recovered from post-consumer tyres, *Eng. Struct.* 45 (2012) 385–395.
- [31] E. Martinelli, A. Caggiano, H. Xargay, An experimental study on the post-cracking behaviour of Hybrid Industrial/Recycled Steel Fiber-Reinforced Concrete, *Constr. Build. Mater.* 94 (2015) 290–298.
- [32] A. Caggiano, H. Xargay, P. Folino, E. Martinelli, Experimental and numerical characterization of the bond behavior of steel fibers recovered from waste tires embedded in cementitious matrices, *Cement Concr. Compos.* 62 (2015) 146–155.
- [33] WIRAND® FIBRE FS7, Maccaferri Technical Data Sheet Rev. 10, Date 08.11.2010.
- [34] FIBROMAC® 12 – Mono-Filamentary Polypropylene Fibre, Maccaferri Technical Data Sheet Rev. 10, Date 08.11.2010.
- [35] EN 12390-4, Testing hardened concrete-compressive strength of test specimens, 2009.
- [36] UNI-11039-1, Steel Fiber Reinforced Concrete-Definitions, Classification and Designation, UNI Editions, Milan, Italy, 2003.
- [37] UNI-11039-2, Steel Fiber Reinforced Concrete – Test Method to Determine the First Crack Strength and Ductility Indexes, UNI Editions, Milan, Italy, 2003.
- [38] E. Cartapati, N. Nisticò, Testing and modelling PAN FR concrete plates damaged by impact loads, in: P. Rossi, G. Chanvillard (Eds.), *Proc. fifth RILEM Symposium on Fibre-Reinforced Concretes (FRC) – BEFIB' 2000*, Lyon, France, ISBN 2-912143-18-7, 2000, pp. 389–398.